Radiation Protection Dosimetry Advance Access published April 16, 2008

Radiation Protection Dosimetry (2008), pp. 1–8 doi:10.1093/rpd/ncn073

RADIATION DOSE FROM A LINEAR SLIT SCANNING X-RAY MACHINE WITH FULL-BODY IMAGING CAPABILITIES

B. J. Irving[1,*], G. J. Maree[2], E. R. Hering[2] and T. S. Douglas[1]
[1]Department of Human Biology, MRC/UCT Medical Imaging Research Unit, University of Cape Town, Cape Town, 7925, South Africa
[2]Division of Medical Physics, Groote Schuur Hospital and University of Cape Town, Cape Town, 7925 South Africa

Received July 9 2007, revised January 31 2008, accepted February 21 2008

Doses for a range of examinations and views using digital X-ray equipment with full-body linear slit scanning capabilities (Statscan) have been compared with those from other published studies. Entrance doses (free-in-air) were measured using a dosimeter, and effective doses were generated using a Monte Carlo simulator. Doses delivered by the linear slit scanning system were significantly lower than those from conventional X-ray equipment. Effective doses were between 9 and 75% of the United Nations Scientific Committee Report on the Effects of Ionising Radiation doses for standard examinations. This dose reduction can be explained by the properties of linear slit scanning technology, including low scatter, beam geometry, the use of a digital detector and the use of higher than usual tube voltages.

INTRODUCTION

Ionising radiation comes from a number of natural and man-made sources. A UK study showed that less than 20% of ionising radiation is artificial[1]; medical radiology constitutes the largest artificial source. The increased use of ionising radiation in medicine worldwide, particularly in computed tomography (CT) scanning, means that there is now a greater need to reduce the radiation dose to patients and medical personnel.

The risks associated with exposure to ionising radiation include those of cancer and genetic effects. There is a linear relationship between radiation dose and the risk solid cancers[2]. Although the risk from an individual radiological examination is small, it is important when considering the number of examinations performed on a population[3].

Slovis[3] suggests that it is important for manufacturers to find ways of reducing dose while maintaining image quality. Studies have shown that linear slit scanning radiography (LSSR) (using a scanning fan beam at a fixed distance from the detector) provides a way of reducing dose without compromising image quality[4,5]. In order to further evaluate and optimise linear slit scanning technology, a dose analysis needs to be completed, including the calculation of effective doses for common X-ray examinations. This study presents the doses for adult patients using a linear slit scanning X-ray imaging system and follows a study on the doses to paediatric patients[6].

*Corresponding author: Benjamin.Irving@uct.ac.za

In this study, the entrance dose was measured 'free-in-air' for routine X-ray examinations (using linear slit scanning technology) in the Trauma Ward at the Groote Schuur Hospital, Cape Town, South Africa. The entrance dose was converted to effective dose (E)[7] using the Monte Carlo simulator PCXMC. Doses have been compared with those reported by the National Radiological Protection Board (NRPB) [now the Health Protection Agency (HPA)][8] and the United Nations Scientific Committee Report on the Effects of Ionising Radiation (UNSCEAR)[9], as well as those obtained in other world wide studies[10–12].

MATERIALS AND METHODS

X-ray equipment

Lodox Systems (Johannesburg, South Africa) have developed low-dose trauma digital X-ray equipment (Statscan) with full-body scanning capabilities[13].

Statscan (Figure 1) uses a rotating anode X-ray tube (1 mm of aluminium equivalent inherent filtration and 1 mm added aluminium filtration) mounted on a C-arm. A collimated fan beam of X-rays is emitted via an adjustable collimator of width 0.4 or 1.0 mm. The half-value layer of the beam is 3.4 mm Al at 80 kV[14]. Fixed to the other end of the C-arm is the X-ray detector unit, comprising scintillator arrays optically linked to charge-coupled devices. The fundamental pixel size of the detectors is 60 μm, with a maximum image size of 12 283 × 8000 pixels. Fourteen bits of contrast resolution can be recorded and a spatial resolution of between 1.04 lp/mm and 5.0 lp/mm can be selected.

Figure 1. Statscan linear slit scanning X-ray machine.

The C-arm can rotate axially around the patient to any angle up to 100° allowing scans at different angles, e.g. lateral and AP. During a scan, the C-arm travels along the table length at speeds ranging between 35 and 140 mm/s. Full-body scans are completed in less than 13 s; the diagnostic image is available for viewing less than 15 s after the end of a scan[15]. The user interface allows the selection of patient size (paediatric, small, medium, large and extra-large) and type of scan; the collimator width and technique factors are automatically selected[13,16]. The technique factors have been selected by Lodox Systems with the intention of optimising image quality and dose. The images can either be viewed on a high-luminance two megapixel monitor or printed onto film.

Entrance dose (free-in-air)

Entrance dose 'free-in-air' (the dose in air without backscatter at the patient surface distance) was measured using a PTW-UNIDOS dosemeter (Freiburg, Germany) and a 30-cm^3 cylindrical ionisation chamber (type 23361) for a range of examinations and views; chest (AP and lateral), abdomen (AP and lateral), pelvis (AP and lateral), skull (AP and lateral), cervical spine (lateral), full spine (lateral) and full body (AP). The doses were corrected for temperature, pressure and kV sensitivity of the ionisation chamber and focus-to-skin distance (FSD).

The uncertainty in the entrance dose measurements was estimated by taking five readings for each of the following: medium-sized patient: chest (AP) and pelvis (AP), and extra-large patient: abdomen (lateral) and skull (AP).

The dose in air was also measured 3.5 cm above the detector (126.5 cm from tube source), with no phantom present, using the same procedure used to measure entrance dose, as well as for the chest AP, abdomen AP and pelvis AP examinations with an Alderson Rando tissue equivalent anthropomorphic phantom present. The scan width used in the phantom measurements was 8.5 cm.

As examinations of large patients are increasing, doses to extra-large patients have also been included in this study. Increased exposure parameters are required for these examinations which can result in a considerable increase in patient dose. The height and weight of a medium-sized patient are assumed to be 174 cm and 71 kg, and of an extra-large patient, 200 cm and 130 kg. The technique factors used for each scan are those set by Lodox and used by Groote Schuur Hospital for each patient size.

Effective dose

Effective dose (E), as defined by the International Commission on Radiological Protection (ICRP) [7], is the sum of the dose to each organ weighted by a tissue weighting factor to take into account the sensitivity of that organ. E is a good indicator of the risk from exposure to ionising radiation.

Entrance dose was converted to E using the Monte Carlo simulator PCXMC (version 1.5.2) released by the Laboratory for Medical Radiation, Finnish Centre for Radiation and Nuclear Safety (Helsinki, Finland). PCXMC uses hermaphrodite

mathematical phantoms and computes dose to 25 organs in the calculation of E [17]; the scan field size was calculated using the internal organs as landmarks. Servomaa and Tapiovaara [17] compared calculations of E from PCXMC with those using the NRPB conversion coefficients. They concluded that there was a good agreement between PCXMC and the NRPB conversion coefficients and that any differences could be explained by statistical error and differences in the models. Similarly, Schultz *et al.*[18] compared calculations of E from PCXMC with those from the general Monte Carlo simulator MCNP. Good agreement was found between the programmes; PCXMC was found to be faster than MCNP.

PCXMC is used for the calculation of E because LSSR has a negligible effect on the conversion coefficients between entrance dose and effective dose. As shown in Figure 2, if the dose-area product (DAP) entering the patient is the same for both conventional radiography and LSSR, the DAP will be the same at any distance. However, the beam area of LSSR only grows perpendicularly to the scanning direction. Thus, the same energy will be imparted by conventional radiography over a slightly larger volume than by LSSR, and there will be a negligible difference in E (for the same entrance dose), affected by a tissue weighting difference from the slightly larger area irradiated in conventional radiography. This was verified by running simulations on PCXMC comparing conventional full-field calculations with summed slice increments at a fixed distance. For example, the scan area for abdomen AP was divided into 186 increments of dimension $0.2 \times 38\ \text{cm}^2$ at a fixed FSD to simulate LSSR. This was compared with the same area exposed by a conventional radiographic unit. The dose for the conventional unit and slit-scanning unit were 8.17 mGy and 8.20 mGy, respectively, using an arbitrary entrance dose; a difference of 0.31%. Thus, PCXMC can be used for the calculation of effective from measured entrance doses in LSSR.

RESULTS

Statscan measurements including entrance dose 'free-in-air', the dose in air at the detector and effective dose (E), for medium-sized and extra-large patients are tabulated (Tables 1 and 2). An estimate of the uncertainty in the measurement of entrance dose at the 95% confidence level was less than $\pm 0.32\%$ and the standard deviation (SD) was less than $\pm 0.26\%$.

Table 3 compares the Statscan doses with those reported by the HPA (previously the NRPB)[8] and the UNSCEAR [9], and from other world wide studies[10–12]. The UNSCEAR doses are those reported for the UK population.

The dose measurements with a phantom present include scatter that does not reach the detector as a result of the detector moving with the beam while the dose meter was stationary. The measurements included in Tables 1 and 2 and the calculation of effective dose are not affected because no phantom is used in these measurements. The air doses above the detector with a standard sized anthropomorphic

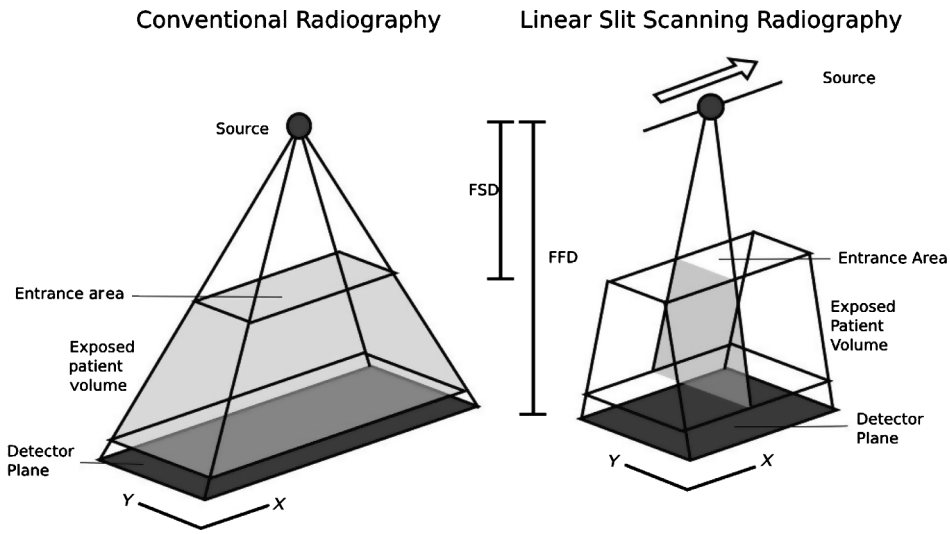

Figure 2. The X-ray beam geometry and exposed volume in conventional radiography and LSSR for the same exposed entrance area.

Table 1. 2007 Statscan doses for medium-sized patients.

Procedure name	Tube voltage (kV)	Slit width (mm)	Focal spot	Tube current (mA)	Scan speed (mm/s)	FSD (cm)	Field size		Air dose at detector (mGy)	Entrance dose (mGy)	*E* (μSv)
							X (cm)	*Y* (cm)			
Full body AP	110	0.4	S	160	140	98.00	37.00	174.00	0.089	0.12	99
Chest AP	100	0.4	S	80	70	99.30	33.50	30.00	0.077	0.099	22
Chest PA[a]	100	0.4	S	80	70	99.30	33.50	30.00	0.077	0.099	15
Chest lateral	120	0.4	S	125	70	72.40	19.00	30.00	0.16	0.28	28
Abdomen AP	100	0.4	S	200	70	98.00	35.00	37.50	0.19	0.24	80
Abdomen lateral	110	1.0	L	200	35	72.40	19.00	34.00	1.1	1.9	160
Pelvis AP	100	0.4	S	200	70	98.00	36.50	28.20	0.19	0.25	60
Pelvis lateral	110	0.4	S	200	70	72.40	20.50	27.00	0.23	0.39	26
Skull AP	110	0.4	S	160	70	93.50	15.90	19.50	0.18	0.24	6.9
Skull lateral	100	0.4	S	160	70	80.40	18.50	20.00	0.15	0.24	6.5
C spine lateral	90	0.4	S	160	70	72.40	11.50	14.00	0.13	0.22	2.1
Full spine lateral	135	1.0	L	200	70	72.40	12.20	71.00	0.75	1.3	190

[a]Chest PA is not used at Groote Schuur Hospital due to trauma setting but is available on Statscan.

Table 2. 2007 Statscan doses for extra-large patients.

Procedure name	Tube voltage (kV)	Slit width (mm)	Focal spot	Tube current (mA)	Scan speed (mm/s)	FSD (cm)	Field size		Entrance dose (mGy)	*E* (μSv)
							X (cm)	*Y* (cm)		
Full body AP	145	0.4	L	200	140	95.00	45.50	200.00	0.24	220
Chest AP	140	0.4	S	160	70	95.00	39.50	35.00	0.36	90
Chest PA[a]	140	0.4	S	160	70	95.00	39.50	35.00	0.36	56
Chest lateral	140	1.0	L	125	70	68.00	23.00	34.50	0.94	80
Abdomen AP	120	1.0	L	200	70	95.00	42.00	42.50	0.83	260
Abdomen lateral	130	1.0	L	200	35	68.00	25.00	37.00	2.6	190
Pelvis AP	120	1.0	L	200	70	95.00	45.00	32.50	0.82	200
Pelvis lateral	130	1.0	L	200	70	68.00	20.00	30.00	1.3	67
Skull AP	120	0.4	L	200	70	93.50	19.60	22.20	0.35	8.6
Skull lateral	110	0.4	L	200	70	80.40	25.00	22.30	0.35	8.9
C spine lateral	110	1.0	L	200	70	68.00	14.50	14.60	0.99	9.5
Full spine lateral	145	1.0	L	200	70	68.00	14.20	79.00	1.5	170

[a]Chest PA is not used at Groote Schuur Hospital due to trauma setting but is available on Statscan.

phantom present are 6 μ Gy for chest AP, 10 μ Gy for abdomen AP and 5 μ Gy for pelvis AP.

DISCUSSION

In order for the effective dose values to be relevant, an image quality assessment must be completed. A study comparing the image quality from Statscan with that of conventional radiography units was carried out at Groote Schuur Hospital[13]. Two radiologists used a seven-point comparative scale to compare the digital images from Statscan with conventional radiographs, for common diagnostic X-ray examinations of 26 patients. The best score from

Table 3. Comparison of 2007 Statscan effective doses (μSv) with those from other studies.

Examination	Statscan (2007)	UNSCEAR (UK) (2000)[9]	NRPB (UK) (2002) [8]	Italy (2005)[10]	Greece (2001)[11]	Bangladesh (2001)[12]
Chest PA	15	20	16	23 ± 8	40	62.2 ± 52.3
Chest lateral	28	40	–	47 ± 26	–	–
Abdomen AP	80	700	760	321 ± 107	–	–
Pelvis AP	60	660	670	386 ± 90	480	626.9 ± 208.9
Skull AP	6.9	30	–	20 ± 6	–	32.6 ± 28.8
Skull lateral	6.5	10	–	11 ± 3	–	24.9 ± 22.2
Full Body AP	99	–	–	–	–	–

Statscan was for the mediastinum with a mean equivalence score of 0.346 (SD = 0.49) and the weakest was for the bony detail (trabeculae) with a mean equivalence score of −0.654 (SD = 0.81). The study concluded that Statscan showed both clinical and radiographic promise. A follow-up study in the USA and South Africa by Boffard *et al.*[19] compared the quality of images between Statscan and conventional radiography units. Radiologists and trauma surgeons analysed images from 115 adult trauma patients. The study concluded that the same amount of information was obtained from Statscan and conventional radiography images and that for the AP plane, Statscan images can replace conventional images[19]. Further evaluation has also demonstrated Statscan's utility in the adult and the paediatric trauma settings[20,21].

At Groote Schuur Hospital, Statscan is used in a trauma setting where patients cannot be turned and an AP instead of a PA projection is used for imaging the chest; a PA projection can be used on Statscan for patients that can be turned. Using a chest PA instead of a chest AP on Statscan reduces *E* by 32% for a medium patient and by 38% for an extra-large patient (See Tables 1 and 2). Chest PA should, therefore, be used wherever possible on Statscan.

Table 3 shows that, for most examinations, the doses from Statscan are considerably lower than those obtained by the UNSCEAR[9], the NRPB[8] and other published studies[10–12]. Examinations that usually have a high dose using conventional X-ray machines are particularly low by comparison. One example is the AP pelvis examination; *E* from Statscan is 9% of the UNSCEAR dose. Thus, more than 10 AP pelvis X-rays can be taken for the same dose as one X-ray on a conventional X-ray machine. A more tangible comparison is that of a return flight from Johannesburg to London which has an effective dose of roughly 75 μSv[1] compared with a Statscan pelvis examination of 60 μSv. Full-body scanning is a key feature of linear slit scanning; *E* from an AP full-body scan is about 14% of an AP abdomen X-ray on a conventional X-ray machine[9]. The dose reduction reported in this study for adult examinations is consistent with that reported by Maree *et al.* [6] for paediatric examinations.

Doses for extra-large patients are greater than the doses for medium patients, as expected, due to higher values kV and mA required for penetration of larger patients. On average, doses for extra-large patients are double the doses for medium-sized patients.

The low effective doses reported, for most examinations, from LSSR can be explained by: the use of a digital detector, the low scatter to primary ratio (SPR) of slit scanning radiography, the geometry of LSSR and the use of higher than usual tube voltages. This discussion extends the reasoning introduced by Potgieter *et al.*[4].

Potgieter *et al.*[4] approximate the dose reduction from the use of an efficient digital detector in Statscan to be 50%, due in part to better detective quantum efficiency (DQE) of digital detectors compared with screen film. However, there will not be any substantial dose reduction due to the detector when Statscan is compared with radiography systems with equivalent digital detectors.

Slit scanning offers a greatly reduced SPR compared with conventional radiography, thus making the use of an antiscatter grid unnecessary[22–24]. The SPR from Statscan with a 20 cm water phantom present was found to have a linear dependence on the precollimator slit width, with an SPR of 0.06 at 0.5 mm and an SPR of 0.1 at 1.0 mm[22]. While, Court and Yamazaki[25] found scatter fractions of between 0.3 and 0.7 (equivalent to an SPR of between 0.4 and 2.3) for a conventional digital radiography unit with various grids and a 15-cm perspex phantom present. This considerable difference in scatter between slit scanning radiography and conventional units with a grid is in agreement with other studies. Barnes *et al.*[24] found that the SPR of a slot scanning chest unit with a precollimator of 0.5 mm was 0.03 which they report as 30 times lower than conventional radiography with a grid. Samei *et al.* [23] also report considerable scatter reductions from slot scanning compared with the use of a grid with conventional full-field radiography.

While still having a lower SPR than conventional radiography, the use of a 1-cm wide precollimator in Samei *et al.*'s study means that a larger SPR is reported compared with other slot scanning radiography units[22,23]. Linear slit scanning and slot scanning are, therefore, very effective methods for scatter reduction.

The use of an antiscatter grid means that a greater dose is required for the examination due to the attenuation of primary radiation. There is large variation in primary transmission for different grids due to the grid characteristics and the tube voltage used in the examination. Studies have found the primary transmission of radiation to vary approximately between 45 and 75%[25–27]. On Statscan, however, no grid is necessary and the ratio between the precollimator and postcollimator is chosen so that the entire primary beam is detected [14]. Thus, there is a 25 to 55% reduction in dose for slit scanning compared with full field from not using a grid.

Detector DQE is used as a measure of the performance of the detector. System (or Effective) DQE, however, takes into account the performance of the whole system including SPR, primary beam transmission and detector performance [23]. Scheelke *et al.* [22] found that for LSSR the system DQE was approximately four times higher than for conventional radiography due to the SPR, transmission and detector DQE described above.

The beam geometry of LSSR also contributes to a lower dose. Figures 2 and 3 show the differences in the beam geometry for linear slit scanning X-ray machines and conventional full-field X-ray machines. In conventional radiography, increasing the distance from the source (r) increases the beam area in both X and Y direction, explaining the $1/r^2$ dose attenuation with r. For LSSR, the dose is proportional to $1/r$ because the beam area only increases in the non-scanning direction (Y) with increasing r[4]. This is verified experimentally by Potgieter *et al.*[4] as well as in this study. When compared with the entrance dose, the dose in air measured at the detector (without a phantom present) shows very good agreement to the $1/r$ dose attenuation of LSSR (see Table 1). As a result of the difference in attenuation, a higher entrance dose is required in conventional radiography in order to obtain the same beam intensity at the detector. Assuming a typical FSD of 90 cm and an FFD of 130 cm this leads to an entrance dose reduction of 30% and an effective dose reduction of 15% for the same patient volume exposed (see Appendix).

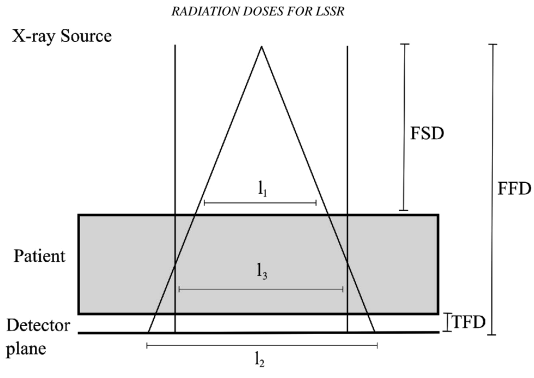

Figure 3. The difference in X-ray beam geometry between conventional full field and LSSR in the scanning direction.

Other factors that also contribute to a lower dose include higher kVs used compared with conventional examinations. There is also the possibility that more quantum mottle is being accepted by radiologists in the image quality studies because quantum mottle is difficult to identify.

Unlike the considerable dose reductions of other examinations, chest examinations show doses only slightly lower than conventional examinations. Potgieter *et al.*[4] explain this in terms of much lower scatter in the chest resulting in less of a difference in the system DQE between LSSR and conventional radiography. Samei *et al.*[23] verify this when comparing slot scanning and conventional radiography in regions of different density in the chest. They show the denser the region, the larger the difference in system DQE between slot scanning and conventional radiography. Chest examinations also generally use a much larger FSD. This results in less of a dose saving due to the beam geometry of LSSR (See Appendix). Statscan also uses a higher kV for most examinations except the chest where high kV examinations are common.

CONCLUSION

In this study, doses for a range of examinations and views using digital X-ray equipment with full-body linear scanning capabilities (Statscan) have been compared with those from other published studies. The results show that doses are considerably lower than those from conventional X-ray equipment for all examinations except the chest. Effective doses were between 9 and 75% of the UNSCEAR doses for standard examinations. This dose reduction can be explained by the properties of linear scanning technology. The low dose along with the full-body imaging capability makes linear scanning technology a useful tool in the trauma environment.

FUNDING

National Research Foundation of South Africa to BJ; Technology and Human Resources for Industry Programme/ Lodox Programme to BJ.

APPENDIX: DOSE REDUCTION FROM THE BEAM GEOMETRY OF LSSR

A derivation is provided to explain dose saving due to the beam geometry of LSSR. The reduction in effective dose in LSSR compared with conventional radiography is obtained for the same dose at the detector.

As shown in Figure 2, the cross-sectional area of the beam increases in both the X and Y directions with increasing distance from the source for conventional radiography, while for LSSR the beam only increases in the non-scanning direction (Y).

As shown in Figure 3, the beam width at the detector is related to the width of the beam at the entrance area by

$$l_2 = \frac{\mathrm{FFD}}{\mathrm{FSD}} l_1 \tag{A.1}$$

where l_1 is the width at the entrance area, l_2 is the width at the detector plane, FFD is the film-focus distance and FSD is the focus-to-skin distance.

Therefore, for conventional radiography, the cross-sectional area of the beam at the detector is

$$A_2 = \left(\frac{\mathrm{FFD}}{\mathrm{FSD}}\right)^2 A_1 \tag{A.2}$$

where A_1 is the beam area at skin entrance and A_2 is the beam area at the detector.

For an LSSR unit, the area does not increase in the scanning direction, therefore

$$A_2 = \left(\frac{\mathrm{FFD}}{\mathrm{FSD}}\right) A_1 \tag{A.3}$$

Considering only the geometry (i.e. in a vacuum), the DAP remains constant at any distance from the detector. Thus, because the DAP remains constant but the area increases, the dose in air(D_{A2}) at the detector is related to the entrance dose in air (D_{A1}) by

$$D_{A2} = D_{A1}\left(\frac{\mathrm{FSD}}{\mathrm{FFD}}\right)^2 \tag{A.4}$$

for conventional radiography and by

$$D_{A2} = D_{A1}\left(\frac{\mathrm{FSD}}{\mathrm{FFD}}\right) \tag{A.5}$$

for LSSR[4].

Thus, for LSSR the entrance dose in air can be reduced by a factor of

$$\left(\frac{\mathrm{FSD}}{\mathrm{FFD}}\right) \tag{A.6}$$

for the same D_A at the detector.

In order to calculate the effective dose saving, the same exposed patient volume must be considered (see Figure 3). Due to the beam geometry, a larger entrance area needs to be exposed for LSSR to obtain the same exposed patient volume and, therefore, the width of the scan needs to be increased by Δ to obtain the same volume.

$$\Delta = \frac{1}{2} l_1 \left(\frac{\mathrm{FFD} - \mathrm{TFD}}{\mathrm{FSD}} - 1\right) \tag{A.7}$$

where TFD is the table to film distance.

Thus, the new scan length in terms of l_1 is

$$l_3 = \frac{1}{2} l_1 \left(\frac{\mathrm{FFD} - \mathrm{TFD}}{\mathrm{FSD}} + 1\right) \tag{A.8}$$

where l_3 is the scan length required by LSSR to obtain the same geometrically exposed volume as conventional full-field radiography.

The increase in exposed entrance area is therefore

$$\frac{1}{2}\left(\frac{\mathrm{FFD} - \mathrm{TFD}}{\mathrm{FSD}} + 1\right) \tag{A.9}$$

If only the geometry is considered and, therefore, assuming that the effective dose weighting factors remain the same, the change in effective dose will be proportional to the change in the entrance area (Equation A.9) as well as the change in entrance dose (Equation A.6).

Thus,

$$E_{\mathrm{LSSR}} = E_{\mathrm{conv}}\left(\frac{\mathrm{FSD}}{\mathrm{FFD}}\right) \times \frac{1}{2}\left(\frac{\mathrm{FFD} - \mathrm{TFD}}{\mathrm{FSD}} + 1\right) \tag{A.10}$$

A simplification can be made by assuming that TFD $<<$ FFD, then:

$$E_{\mathrm{LSSR}} = E_{\mathrm{conv}}\left(\frac{\mathrm{FSD}}{\mathrm{FFD}}\right)\frac{1}{2}\left(\frac{\mathrm{FFD}}{\mathrm{FSD}} + 1\right) \tag{A.11}$$

$$= E_{\mathrm{conv}}\frac{1}{2}\left(1 + \frac{\mathrm{FSD}}{\mathrm{FFD}}\right) \tag{A.12}$$

where E_{LSSR} is the effective dose for a LSSR unit and E_{conv} is the effective dose from a conventional full-field radiography unit. Thus, the smaller the FSD and the larger the FFD, the greater the dose saving for LSSR. An increased TFD will also lead to a lower dose relative to conventional radiography.

REFERENCES

1. Watson, S., Jones, A., Oatway, W. and Hughes, J. *Ionising Radiation Exposure of the UK Population: 2005 Review*, HPA-RPD-001. HPA Chilton, U.K (2005).
2. Ron, E. *Ionizing radiation and cancer risk: evidence from epidemiology.* Pediatr. Radiol. **32**, 232–237 (2002).
3. Slovis, T. *CT and computed radiography: the pictures are great, but is the radiation dose greater than required*? Am. J. Roentgenol. **179**, 39–41 (2002).
4. Potgieter, J., de Villiers, M., Scheelke, M. and de Jager, G. *An explanation for the extremely low, but variable radiation dosages measured in a linear scanning radiography system*. In: Medical Imaging 2005: Physics of Medical Imaging. **5745**, pp. 1138–1145 (2005).
5. Barnes, G., Wu, X. and Sanders, P. *Scanning slit chest radiography: a practical and efficient scatter control design*. Med. Phys. **190** ,525–528 (1994).
6. Maree, G., Irving, B. and Hering, E. *Paediatric dose measurement in a full-body digital radiography unit*. Pediatr. Radiol. **37**, 990–997 (2007).
7. International Commission on Radiological Protection. *1990 Recommendations of the ICRP.* Ann. ICRP (Oxford, UK: Pergamon Press) **21** (1991).
8. Hart, D. and Wall, B. *Radiation Exposure of the UK Population from Medical and Dental x-ray Examinations*, NRPB-W4 (Chilton, UK: NRPB) (2002).
9. United Nations Scientific Committee on the Effects of Atomic Radiation. *UNSCEAR 2000 Report to General Assembly.* (New York: UNSCEAR) (2000).
10. Compagnone, G., Pagan, L. and Bergamini, C. *Effective dose calculations in conventional X-ray diagnostic examinations for adult and paediatric patients in a large Italian hospital*. Radiat. Prot. Dosim. **114**, 164–167 (2005).
11. Papadimitriou, D., Perris, A., Molfetas, M., Panagiotakis, N., Manetou, A., Tsourouflis, G., Vassileva, J., Chronopoulos, P., Karapanagiotou, O. and Kottou, S. *Patient dose, image quality and radiographic techniques for common x ray examinations in two Greek hospitals and comparison with European guidelines.* Radiat. Prot. Dosim. **95**, 43–48 (2001).
12. Begum, Z. *Entrance surface, organ and effective doses for some of the patients undergoing different typed of x ray procedures in Bangladesh*. Radiat. Prot. Dosim. **95**, 257–262 (2001).
13. Beningfield, S., Potgieter, H., Nicol, A., van As, A., Bowie, G., Hering, E. and Latti, E. *Report on a new type of trauma full-body digital X-ray machine.* Emerg. Radiol. **10**, 23–29 (2003).
14. Scheelke, M. *System characterisation of a full body slit scanning radiography machine: theory and experiment*. Masters thesis, University of Cape Town (2005).
15. Lodox Systems. *Statscan critical imaging system - product specifications and physical dimensions.* Lodox, technical report.
16. Miller, L., Mirvis, S., Harris, L. and Haan, J. *Total-body digital radiography for trauma screening: initial experience.* Appl. Radiol. **33**, 8–14 (2004).
17. Servomaa, A. and Tapiovaara, M. *Organ dose calculation in medical x-ray examinations by the program PCXMC.* Radiat. Prot. Dosim. **80**, 213–219 (1998).
18. Schultz, F., Geleijns, J., Spoelstra, F. and Zoetelief, J. *Monte Carlo calculations for assessment of radiation dose to patients with congenital heart defects and to staff during cardiac catheterizations.* Br. J. Radiol. **76**, 638–647 (2003).
19. Boffard, K. D., Goosen, J., Plani, F., Degiannis, E. and Potgieter, H. *The use of low dosage X-ray (Lodox/Statscan) in major trauma: comparison between low dose X-ray and conventional X-ray techniques.* J. Trauma. **60**, 1175–1181 (2006).
20. Douglas, T. S., Sanders, V., Pitcher, R. and van As, A. B. *Early detection of fractures with low-dose digital x-ray images in a pediatric trauma unit*. J. Trauma. (in press). Doi: 10.1097/01.ta.0000198534.47134.bc.
21. van As, A. B., Douglas, T. S., Kilborn, T., Pitcher, R. and Rode, H. *Multiple injuries diagnosed using full-body digital x-ray.* J. Pediatr. Surg. **41**, E25–E28 (2006).
22. Scheelke, M., Potgieter, J. and de Villiers. *System characterization of the STATSCAN full body slit scanning radiography machine: theory and experiment*. Medical Imaging 2005: Physics of Medical Imaging (SPIE), **5745**, 1179–1190 (2005).
23. Samei, E., Lo, J., Yoshizumi, T., Jesneck, J., Dobbins, J., Floyd, C., McAdams, H. and Ravin, C. *Comparative scatter and dose performance of slot-scan and full-field digital chest radiography systems.* Radiol. **235**, 940–949 (2005).
24. Barnes, T., Sones, R. and Tesic, M. *Digital chest radiography: performance evaluation of a prototype Unit*. Radiol. **154**, 801–806 (1985).
25. Court, L. and Yamazaki, T. *Technical note: a comparison of antiscatter grids for digital radiography.* Brit. J. Radiol. **77**, 950–952 (2004).
26. Kalender, W. *Calculation of x-ray grid characteristics by Monte Carlo methods.* Phys. Med. Biol. **27**, 353–361 (1982).
27. Chan, H. and Doi, K. *Investigation of the performance of antiscatter grids: Monte Carlo simulation studies.* Phys. Med. Biol. **27**, 785–803 (1982).